Hindawi
Shock and Vibration
Volume 2018, Article ID 6378023, 16 pages
https://doi.org/10.1155/2018/6378023

Research Article

Multimode Coordination Control of a Hybrid Active Suspension

Fa-Rong Kou, Dong-Dong Wei, and Lei Tian

School of Mechanical Engineering, Xi'an University of Science and Technology, Xi'an, Shaanxi, China

Correspondence should be addressed to Dong-Dong Wei; 1462739700@qq.com

Received 1 July 2018; Revised 23 October 2018; Accepted 11 November 2018; Published 16 December 2018

Academic Editor: Francesco Braghin

In order to effectively realize the damping control and regenerative energy recovery of vehicle suspension, a new kind of hybrid active suspension structure with the ball screw actuator and magnetorheological (MR) damper is put forward. Firstly, for the analysis of the suspension performance, a quarter dynamic model of vehicle hybrid suspension is established, and at the same time, the mathematical models of MR damper and ball screw actuator are founded. Secondly, the active mode with damping switching control of the hybrid suspension and the semiactive mode with feedback adjustment of the electromagnetic damping force of the hybrid suspension are analyzed. Then, the multimode coordinated control system of the hybrid suspension is designed. Under the cyclic driving condition, the damping performance and energy consumption characteristics of the hybrid suspension are simulated by MATLAB/Simulink software. Finally, the bench tests of the hybrid suspension system are done. The simulation and experimental results show that compared with passive suspension, the root mean square of the sprung mass acceleration of the hybrid suspension with the active mode and semiactive mode is, respectively, reduced by 39% and 16% under the random road. The damping effect of the hybrid suspension system is obvious.

1. Introduction

A controllable actuator is used to replace the corresponding components of original passive suspension, which is named as an active suspension. Active suspension can adjust suspension stiffness and damping, according to changes in the current road conditions, to improve vehicle riding comfort and handling stability [1, 2]. However, the active suspension actuator needs to consume a large amount of external energy and it reduces the economic performance of the vehicle [3–5].

In recent years, domestic and overseas scholars have been studying how to reduce the energy consumption of active suspension from two aspects. On the one hand, the regenerative energy active suspension structures are used to recover vibration energy, which is used for the active control of the suspension. For example, Nakano et al. [6, 7] used two linear motor actuators for active control and vibration energy recovery, respectively, and as a result, the active suspension system was self-powered. Huang et al. [8, 9] proposed a new type of energy-regenerative electromagnetic suspension structure with a parallel-type ball screw actuator, which included a fully active mode and semiactive mode. Huang et al. [10] designed a regenerative energy active suspension system and analyzed the power conversion process of the suspension system, and the simulation results show that under regenerative energy and active mode switching control, the suspension system was self-powered. However, when the regenerative energy active suspension is used to recover vibration energy of the suspension, the active control of the suspension cannot be realized, so the riding comfort and handling and stability of vehicle will be reduced.

On the other hand, domestic and overseas scholars researched how to reduce the energy consumption of active suspensions by improving the suspension structures and optimizing the structural parameters of active suspensions. For example, Ebrahimi et al. [11] proposed a hybrid electromagnetic shock absorber, which was applied to an active suspension, developed a prototype of the shock absorber, and carried out the experimental researches; then, the tests show that the electromagnetic shock absorber was beneficial to reduce the energy consumption of the active suspension. Tang et al. [12] proposed an active suspension structure with paralleled three-gear variable damper and designed the switching control strategy of the damper, and the simulation results show that, for the suspension structure, the energy

consumption under the active control mode was reduced. Wang et al. [13, 14] proposed a hybrid suspension structure with parallel damping variable shock absorber, designed the variable damping of the suspension in different working modes, and carried out the simulations and experimental research studies; the results show that for the suspension structure, the energy consumption under the active control mode was reduced. However, for the research studies on the active suspension structure and the structural parameters optimization, the energy consumption of the variable damping shock absorber is not taken into account, and the impacts of the energy consumption on the economic performance of the suspension system are not analyzed. Moreover, under different vehicle speeds, the impacts of different damping values of the variable damping shock absorber on vehicle ride comfort, handling and stability, and economic performance are not analyzed.

For the MR damper, the continuous variable characteristics of the damping coefficient can be achieved by controlling the magnetic field strength of the MR fluid [15–17]. A new kind of hybrid active suspension structure with ball screw actuator and MR damper is put forward. Moreover, in order to ensure high response speed of the hybrid active suspension, a sky-hook algorithm, which is easy to operate, fast and robust in response, is applied [18–20]. And the semiactive mode and active mode of the hybrid suspension are analyzed under the class B road surface. At the same time, the multimode coordinated control system of the hybrid suspension is designed. Then, the damping performance and energy consumption characteristics of the hybrid suspension under the cyclic driving condition are simulated, and the bench tests of the hybrid suspension system are done.

2. Structure and Principle of the Hybrid Active Suspension

The structure of the hybrid active suspension system is shown in Figure 1. It is mainly composed of spring, MR damper, ball screw actuator, controller, battery, corresponding signal detection device, and so on.

The controller performs semiactive control or active control of the hybrid suspension system by detecting and judging the relevant signals. When the hybrid suspension is semiactively controlled, the controller detects the sprung mass acceleration in real time by the sprung mass acceleration sensor, and the semiactive control force of the hybrid suspension is obtained through the sky-hook algorithm. The controller adjusts the controllable current to change the magnetic field strength of the MR fluid. Then, the output damping force of the MR damper is changed, and the semiactive control of the suspension is realized. At the same time, the ball screw actuator transforms the up and down motion of the suspension into the rotation of the motor, and then, the motor generates electric energy which is stored in the battery.

When the hybrid suspension is actively controlled, the controller detects the sprung mass acceleration in real time by the sprung mass acceleration sensor, and the active control force of the hybrid suspension is obtained through the sky-hook algorithm. The controller adjusts the controllable current to change the motor output torque. The motor transforms the rotation motion into the up and down motion, and the active control of the suspension is realized. At this time, the energy consumed by the ball screw actuator is supplied by the battery. And when the hybrid suspension is actively controlled, the controller detects the running speed of vehicle and controls the input current of the MR damper according to different vehicle speed values. It makes the MR damper produce a damping value that matches the vehicle speed. In the semiactive and active control of the suspension, the energy consumed by the MR damper is all provided by the battery.

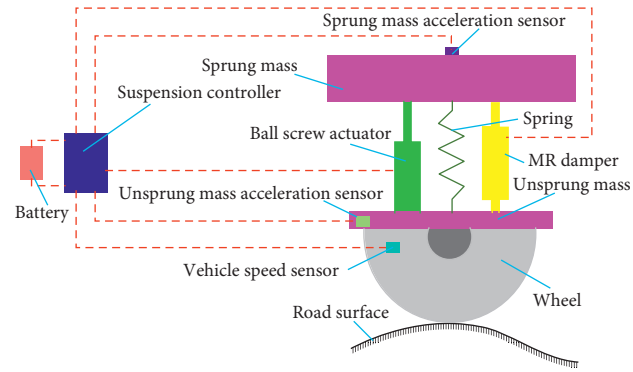

Figure 1: Structure of the hybrid active suspension.

3. Modeling of Hybrid Active Suspension Dynamic Model

3.1. Dynamic Model of Hybrid Active Suspension. In this paper, a quarter vehicle dynamic model of the hybrid active suspension is established and shown in Figure 2.

Based on Newton's laws of motion, the dynamic motion equations for the quarter vehicle suspension can be expressed as

$$\begin{cases} m_s\ddot{x}_2 + k_s(x_2 - x_1) + c_s(\dot{x}_2 - \dot{x}_1) = F, \\ m_u\ddot{x}_1 - k_s(x_2 - x_1) - c_s(\dot{x}_2 - \dot{x}_1) + k_t(x_1 - z) = -F. \end{cases} \tag{1}$$

The state variable and the output vector are selected as follows:

$$\begin{aligned} \mathbf{X} &= [x_2 - x_1 \ \dot{x}_2 \ x_1 - z \ \dot{x}_1]^T, \\ \mathbf{Y} &= [\ddot{x}_2 x_2 - x_1 k_t (x_1 - z) \ \dot{x}_1]^T, \end{aligned} \tag{2}$$

where m_s is sprung mass; m_u is unsprung mass; k_s is spring stiffness coefficient; F is control force of suspension (especially F_b is semiactive control force and F_z is active control force); k_t is tire stiffness coefficient; z is displacement of road input; x_2 is displacement of sprung mass; x_1 is displacement of unsprung mass; and c_s is damping coefficient of MR damper.

Then, the state-space equations of suspension system can be described as follows:

$$\begin{cases} \dot{\mathbf{X}} = \mathbf{AX} + \mathbf{BU}, \\ \mathbf{Y} = \mathbf{CX} + \mathbf{DU}, \end{cases} \tag{3}$$

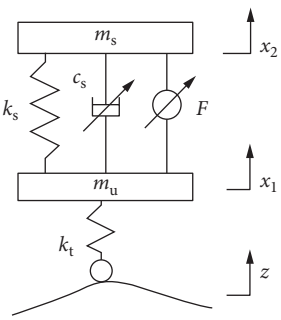

Figure 2: Dynamic model of 2 DOF hybrid active suspension.

where $\mathbf{A}, \mathrm{B}, \mathbf{C}$, and $\mathbf{D}$ are the state matrix, input matrix, output matrix, and transfer matrix, respectively. When the control input force F is 0, it becomes passive suspension.

$$\mathbf{A} = \begin{bmatrix} 0 & 1 & 0 & -1 \\ -\frac{k_s}{m_s} & -\frac{c_s}{m_s} & 0 & \frac{c_s}{m_s} \\ 0 & 0 & 0 & 1 \\ \frac{k_s}{m_u} & \frac{c_s}{m_u} & -\frac{k_t}{m_u} & -\frac{c_s}{m_u} \end{bmatrix},$$

$$\mathbf{B} = \begin{bmatrix} 0 & 0 \\ 0 & \frac{1}{m_s} \\ -1 & 0 \\ 0 & -\frac{1}{m_u} \end{bmatrix},$$

$$\mathbf{X} = \begin{bmatrix} -\frac{k_s}{m_s} & -\frac{c_s}{m_s} & 0 & \frac{c_s}{m_s} \\ 1 & 0 & 0 & 0 \\ 0 & 0 & k_t & 0 \\ 0 & 0 & 0 & 1 \end{bmatrix}, \tag{4}$$

$$\mathbf{D} = \begin{bmatrix} 0 & \frac{1}{m_s} \\ 0 & 0 \\ 0 & 0 \\ 0 & 0 \end{bmatrix},$$

$$\mathbf{U} = \begin{pmatrix} \dot{z} \\ F \end{pmatrix}.$$

A filtered white noise is adopted as the road surface input model as follows:

$$\dot{z}(t) = -2\pi f_0 z(t) + 2\pi\sqrt{G_0 u}\,\omega(t), \tag{5}$$

where G_0 is the coefficient of road irregularity; f_0 is lower cutoff frequency; u is vehicle speed; and $\omega(t)$ is unit white noise.

The simulation parameters of the hybrid suspension are listed in Table 1.

3.2. MR Damper Mathematical Model. Ignoring the friction and fluid inertia of the MR fluid, the damping force model of the MR damper under mixed operation mode is given as follows [21]:

$$F_a = -\left(\frac{24\eta A_p^2 l}{bh^3} + \frac{2\eta bl}{h}\right)(\dot{x}_2 - \dot{x}_1) - \left(\frac{4lA_p}{\eta} + 2bl\right)\tau_y, \tag{6}$$

where F_a is MR damper output damping force; η is fluid dynamic viscosity; l is the working plate length; h is the working plate distance; τ_y is MR fluid shear stress; A_p is piston effective area; and b is the working plate width.

According to formula (6), the damping force of the MR damper includes the viscous damping force F_n, which has a function relationship with the piston speed of the MR damper, and coulomb damping force F_k, which has a function relationship with the control current of the MR damper. So formula (6) can be transformed into

$$F_a = -c_e(\dot{x}_2 - \dot{x}_1) + \left(a_1 I_k^2 + a_2 I_k^2 + a_3\right)\mathrm{sgn}(\dot{x}_2 - \dot{x}_1), \tag{7}$$

where c_e, a_1, a_2, and a_3 are polynomial coefficients and I_k is control current of the MR damper.

From formulae (6)~(7), because the viscous damping force F_n does not consume energy, it can be equivalent to the damping force produced by the traditional hydraulic shock absorber. The variable damping force of the hybrid active suspension is the coulomb damping force F_k, which is achieved by adjusting I_k.

In the semiactive control of the hybrid suspension, the instantaneous energy consumption power and the energy consumption of the MR damper are expressed as

$$P_b = F_k \cdot \frac{(\dot{x}_2 - \dot{x}_1)}{\eta_b}, \tag{8}$$

$$W_b = \int_0^t P_b\, dt, \tag{9}$$

where η_b is work efficiency of MR damper; P_b is the MR damper instantaneous energy consumption power of the hybrid suspension in semiactive control; and W_b is the MR damper energy consumption of the hybrid suspension in semiactive control.

In the active control of the hybrid suspension, the output damping force of the MR damper is expressed as

Table 1: Simulation parameters of the hybrid suspension.

Parameters	Values
Lower cutoff frequency (Hz)	0.1
Road irregularities coefficient (m^3)	64×10^{-6}
Sprung mass (kg)	38
Unsprung mass (kg)	210
Spring stiffness coefficient (kN/m)	22
Tire stiffness coefficient (kN/m)	200

$$c_s = c_0 + c_k,$$
$$c_0 = \frac{F_n}{(\dot{x}_2 - \dot{x}_1)}, \quad (10)$$
$$c_k = \frac{F_k}{(\dot{x}_2 - \dot{x}_1)},$$

where c_0 is viscous damping of the MR damper and c_k is variable damping of the MR damper.

In the active control, the instantaneous energy consumption power and the energy consumption of the MR damper are expressed as

$$P_c = \frac{(c_s - c_0) \cdot (\dot{x}_2 - \dot{x}_1)^2}{\eta_b}, \quad (11)$$

$$W_c = \int_0^t P_c \, dt, \quad (12)$$

where P_c is the MR damper instantaneous energy consumption power of the hybrid suspension in active control and W_c is the MR damper energy consumption of the hybrid suspension in active control.

The single rod MR damper is used in this paper, and it is shown in Figure 3.

By carrying out the characteristics test of the MR damper and analyzing the test data, the relation diagrams of the damping force-velocity curves of the MR damper are obtained and shown in Figure 4.

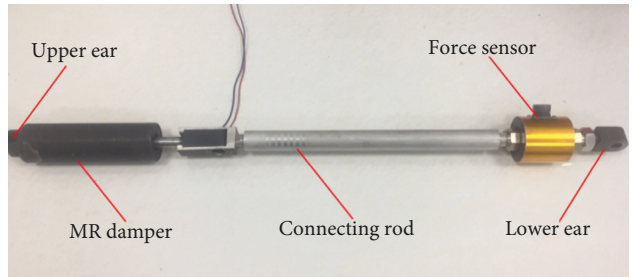

Figure 3: The MR damper prototype.

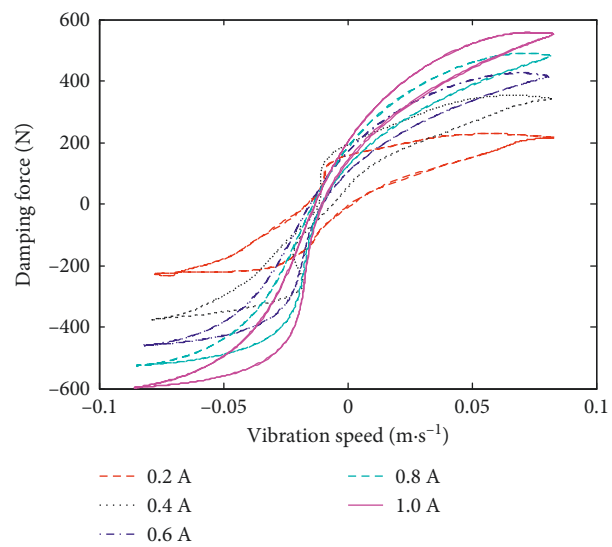

Figure 4: The damping force-velocity curves of the MR damper.

3.3. Ball Screw Actuator Mathematical Model

3.3.1. The Characteristics of Ball Screw Actuator. The ball screw actuator is used not only to realize the active control of the hybrid suspension but also to recover the regenerative energy of the hybrid suspension, the characteristics of which have a great influence on the performance of the hybrid suspension.

The characteristics of the ball screw actuator is mainly affected by the back-EMF coefficient k_e and electric torque coefficient k_T of the motor, but the nonlinear characteristics of the motor make k_e and k_T vary with the speed of the motor [22, 23]. It is necessary to gain the relationship between k_e, k_T, and the motor speed by the motor test if a precise mathematical model of the ball screw actuator is established.

The prototype of the ball screw actuator is shown in Figure 5. It is made up of brushless DC motor, ball screw, upper and lower ears, force sensor, and so on.

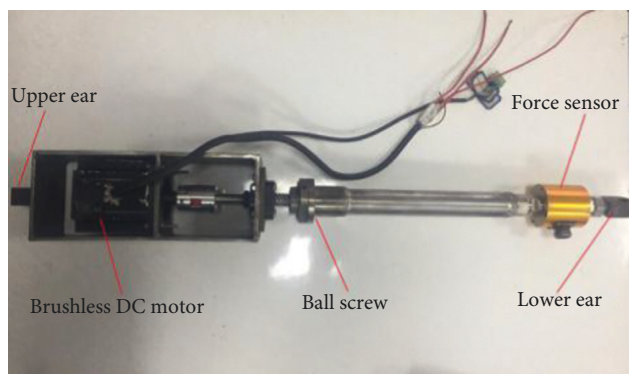

Figure 5: The ball screw actuator.

In this paper, the peak value of counter electromotive force of the motor at different rotating speeds is measured by the test. At different rotating speeds, the fitting analyses of the peak value are carried out, and the result is shown in Figure 6.

The peak of counter electromotive force of the motor and the back-EMF coefficient meet the following relationships:

$$k_e = \frac{V_{max}}{2\sqrt{2}n}, \quad (13)$$

where V_{max} is the peak of counter electromotive force and n is motor rotating speed.

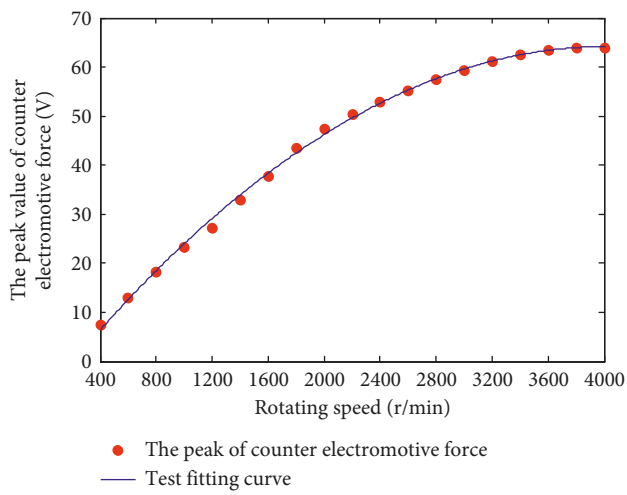

Figure 6: The peak value curve of counter electromotive force of the motor.

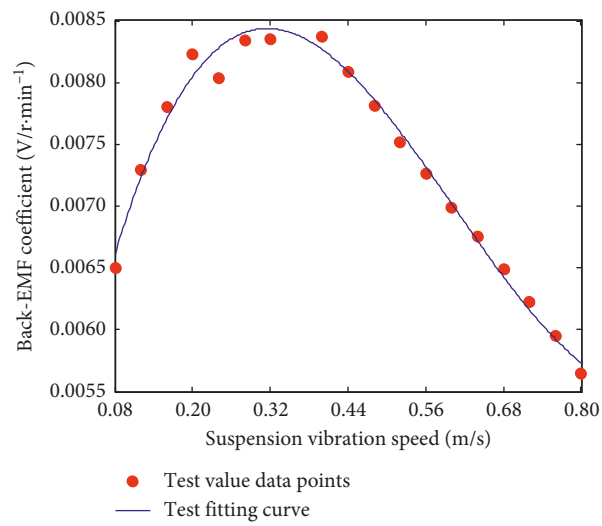

Figure 7: The motor back-EMF coefficient curve.

The vibration velocity of the hybrid suspension and the motor rotating speed meet the following relationships:

$$n = \frac{\Delta v}{L} \cdot 60, \tag{14}$$

$$\Delta v = \dot{x}_2 - \dot{x}_1, \tag{15}$$

where Δv is the suspension vibration velocity and L is ball screw lead.

At different suspension vibration velocity, the motor back-EMF coefficient can be obtained from formulae (13)~(15), and the fitting curve of the motor back-EMF coefficient is shown in Figure 7.

In Figure 7, the fitting relationship between k_e and Δv is expressed as

$$k_e = 0.0299\Delta v^3 - 0.0542\Delta v^2 + 0.0253\Delta v + 0.0049. \tag{16}$$

Then, k_T and k_e meet the following relationships:

$$k_T = \frac{30}{\pi} k_e. \tag{17}$$

The relationship between k_T and Δv can be obtained from formulae (16) and (17).

$$k_T = 0.2855\Delta v^3 - 0.5176\Delta v^2 + 0.2416\Delta v + 0.0468. \tag{18}$$

When testing the active output force of the ball screw actuator, the ball screw actuator is powered by the same 72 V constant voltage source as the battery pack terminal voltage. By adjusting PWM duty ratio, the input voltage and current of the motor are controlled by the controller, and as a result, the output force of the motor is gained. The relationship between the active output force of the ball screw actuator and duty ratio is shown in Figure 8.

From Figure 8, it can be seen that the ball screw actuator has good active output force characteristics, and the nonlinear relationship between the output force and the duty ratio is consistent with the nonlinear characteristics of the motor.

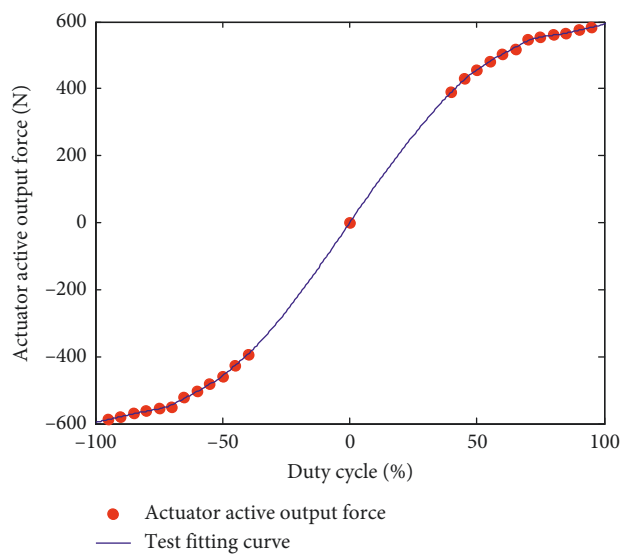

Figure 8: Testing curve of the actuator active output force.

3.3.2. Ball Screw Actuator Mathematical Model. When the motor inductance is ignored, in the active control of the hybrid suspension, input voltage E and the output torque T_m of the motor meet the following relationships:

$$E = u + I_z r, \tag{19}$$

$$T_m = k_T \cdot I_z, \tag{20}$$

$$u = \frac{60(\dot{x}_2 - \dot{x}_1)}{L} \cdot k_e, \tag{21}$$

$$T_m = \frac{F \cdot L}{2\pi}, \tag{22}$$

$$k_e = \frac{k_T \cdot \pi}{30}, \tag{23}$$

where u is induced electromotive force; I_z is motor current; and r is internal resistance of the motor.

In the active control of the hybrid suspension, the instantaneous energy consumption power of the ball screw actuator can be expressed as

$$P_z = \frac{E \cdot I_z}{\eta_z}. \tag{24}$$

The instantaneous energy consumption power and consumption energy can be obtained from formulae (19)~(24) as follows:

$$P_z = \frac{\left[\left(\dot{x}_2 - \dot{x}_1\right) \cdot F + \left(FL/2\pi k_T\right)^2 \cdot r\right]}{\eta_z}, \tag{25}$$

$$W_z = \int_0^t P_z \, dt, \tag{26}$$

where P_z is motor instantaneous energy consumption power; η_z is transfer efficiency of ball screw actuator; and W_z is motor energy consumption.

In the energy regeneration of the hybrid suspension, the electromagnetic damping force generated by the ball screw actuator is expressed as

$$F_s = -\left(\frac{2\pi k_T}{L}\right)^2 \cdot \frac{\left(\dot{x}_2 - \dot{x}_1\right)}{R + r}\eta_z, \tag{27}$$

where F_s is the electromagnetic damping force and R is external resistance of the motor.

The instantaneous energy-regenerative power and regenerative energy of the ball screw actuator can be expressed as

$$P_k = \left(\frac{2\pi k_e}{L}\right)^2 \cdot \frac{\left(\dot{x}_2 - \dot{x}_1\right)^2}{R + r}\eta_z, \tag{28}$$

$$W_k = \int_0^t P_k \, dt, \tag{29}$$

where P_k is instantaneous energy-regenerative power and W_k is regenerative energy.

4. Multimode Coordination Control of Hybrid Active Suspension

4.1. The Active Mode of Damping Switching Control. The sprung mass acceleration is the main evaluation index of vehicle riding comfort, and the dynamic tire load is closely related to vehicle handling and stability. An active control model of the hybrid suspension is established by MATLAB/Simulink software to simulate and analyze the influence of the variable damping for the hybrid active suspension on vehicle riding comfort and handling and stability at different vehicle speeds. During the simulation, the range of vehicle speed v is 0–120 km/h and the vehicle speed is taken every 10 km/h. The variable damping range of the suspension is 200–2000 N·s/m, and the value of the variable damping is taken every interval 100 N·s/m. The simulation time is 10 s, and the value of r is 0.5 Ω. The value of η_z is 0.97, and the value of η_b is 0.98. The value of c_{sky} is 2000 N·s/m.

When the vehicle speed is 30 km/h and 100 km/h, respectively, the RMS of the sprung mass acceleration of the vehicle (a_w) and the RMS of the dynamic tire load (DTL_{rms}) change with the variable damping of the hybrid active suspension, as shown in Figures 9 and 10.

From Figures 9 and 10, it can be seen that when the vehicle speed is 30 km/h, the variable damping values that make a_w of vehicle and DTL_{rms} minimum are 400 N·s/m and 1000 N·s/m, respectively, and when the vehicle speed is 100 km/h, the variable damping values that make a_w of vehicle and DTL_{rms} minimum are 500 N·s/m and 1100 N·s/m, respectively. Therefore, at a certain vehicle speed, the variable damping of the hybrid active suspension cannot make the best of the vehicle riding comfort and handling and stability at the same time.

Suspension performance indexes include the sprung mass acceleration, suspension working space, and dynamic tire load. In this paper, in order to balance vehicle riding comfort and handling and stability, when choosing the variable damping values of the hybrid suspension in the active control, for the sprung mass acceleration, suspension working space, and dynamic tire load of the hybrid active suspension, the quantitative normalizations and comparative analyses are done. That is, at the same vehicle speed, compared with the passive suspension, the improvement amplitudes of each performance index of the hybrid active suspension are multiplied by different quantification factors and summed. And the larger the sum, the better the dynamic performance of vehicle. Among them, the quantification factors of a_w, the RMS value of suspension working space (SWS_{rms}), and DTL_{rms} are 1, 0.2703, and 0.1443, respectively [24, 25]. And when the vehicle speed is 30 km/h and 100 km/h, respectively, the dynamic performance and the active control energy consumption of the hybrid active suspension change with the variable damping, as shown in Figures 11 and 12.

From Figures 11 and 12, when the vehicle speed is 30 km/h, the variable damping value of the hybrid active suspension is 800 N·s/m, which makes the vehicle dynamic performance the best and the active energy consumption the least. When the vehicle speed is 100 km/h, the variable damping value of the hybrid active suspension is 1000 N·s/m, which makes the vehicle dynamic performance the best and active energy consumption the least. Therefore, when the vehicle speed is 30 km/h and 100 km/h, respectively, the optimal damping values of the hybrid active suspension are 800 N·s/m and 1000 N·s/m, respectively. When the vehicle speed is 0–120 km/h, the optimal damping values of the hybrid active suspension at different vehicle speeds are shown in Figure 13. If the damping value which makes the vehicle dynamic performance the best is different from the damping value which makes the active control energy consumption the least, the damping value which makes the vehicle dynamic performance the best is selected as the optimal damping value of the hybrid active suspension at the vehicle speed.

When vehicle is in an accelerating or decelerating state, its speed changes rapidly and the range of change is wide, so the vehicle speed value is not easily detected in real time, and in order to reduce the energy consumption of the hybrid suspension active controlled and to improve the vehicle

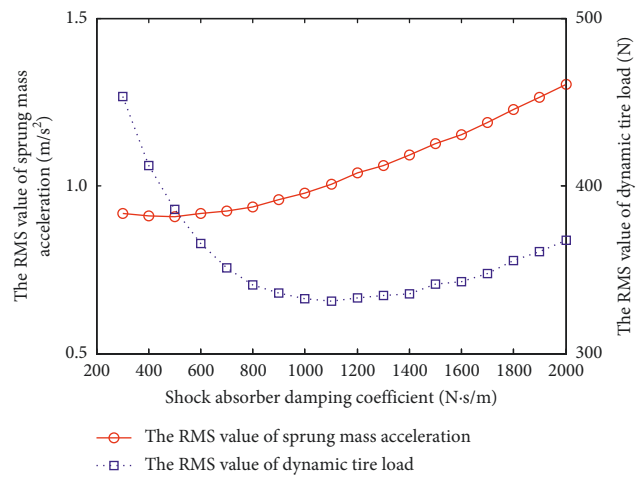

Figure 9: Relationship between the variable damping and the riding comfort, handling, and stability of vehicle at 30 km/h speed.

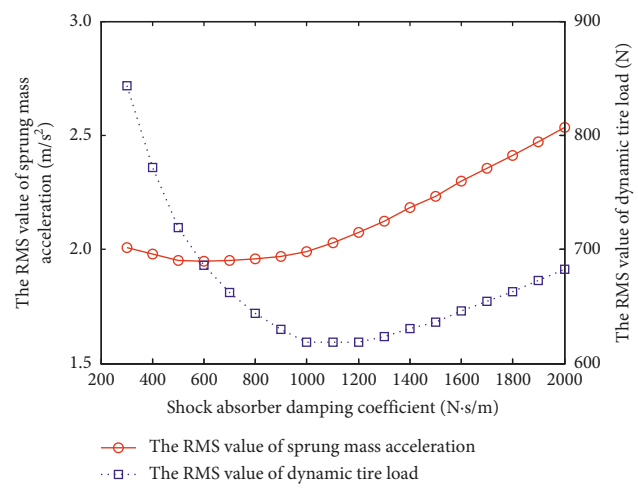

Figure 10: Relationship between the variable damping and the riding comfort, handling, and stability of vehicle at 100 km/h speed.

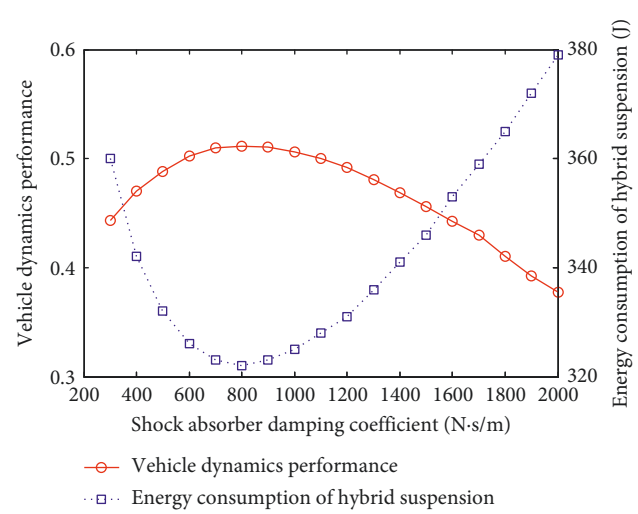

Figure 11: Relationship between the variable damping and vehicle dynamic performance at 30 km/h speed.

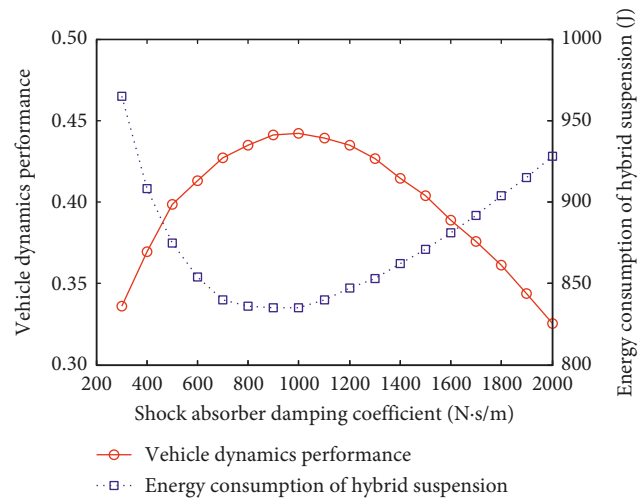

Figure 12: Relationship between the variable damping and vehicle dynamic performance at 100 km/h speed.

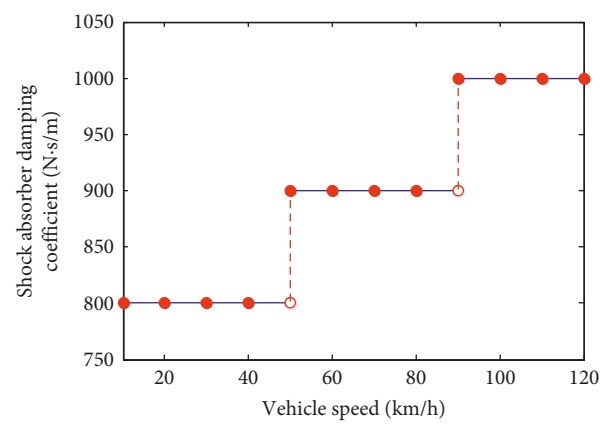

Figure 13: Suspension optimal damping at different speeds.

riding comfort and handling and stability, a variable damping switching control strategy of the hybrid active suspension is designed as follows:

$$\begin{cases} \begin{cases} F_z = -c_{\text{sky}} \cdot \dot{x}_2, \\ c_s = c_0 + c_k, \end{cases} & \dot{v} = 0, \\ \begin{cases} F_z = -c_{\text{sky}} \cdot \dot{x}_2, \\ c_s = c_0, \end{cases} & \dot{v} \neq 0, \end{cases} \tag{30}$$

where $\dot{v}$ is vehicle acceleration and c_{sky} is sky-hook coefficient.

4.2. The Semiactive Mode of Feedback Adjustment of Electromagnetic Damping Force. MR damper can effectively perform semiactive control at $(\dot{x}_2 - \dot{x}_1)\dot{x}_2 > 0$, so the ideal semiactive control state for hybrid suspension is

$$F_b = \begin{cases} -c_{\text{sky}} \cdot \dot{x}_2, & (\dot{x}_2 - \dot{x}_1)\dot{x}_2 > 0, \\ 0, & (\dot{x}_2 - \dot{x}_1)\dot{x}_2 \leq 0. \end{cases} \tag{31}$$

From equation (31), the ideal semiactive control force of the hybrid suspension $-c_{\text{sky}} \cdot \dot{x}_2$ is only related to $\dot{x}_2$ when

the sky-hook coefficient c_{sky} is constant. However, at this time, the ball screw actuator, as a power feeding device, generates the electromagnetic damping force F_s and acts on the suspension, so that the actual semiactive control force of the suspension is different from the ideal semiactive control force $-c_{sky} \cdot \dot{x}_2$. In this paper, the semiactive control model of the hybrid suspension is established, and the change effects of the different output forces on the vehicle riding comfort and handling stability are analyzed by MATLAB/Simulink software. The simulation speed is 70 km/h, the simulation time is 5 s, and the value of R is 0.75 Ω. The damping comparison of the hybrid suspension in semiactive control is shown in Figure 14.

Figure 14 shows that compared with the ideal semiactive control force, the actual semiactive control force of the hybrid suspension fluctuates violently, and the absolute value of the actual semiactive control force is greater than the absolute value of the ideal semiactive control force $|c_{sky} \cdot \dot{x}_2|$ at certain times. And a drastic change in the actual semiactive control force makes the suspension not reach ideal semiactive control effect. Using electromagnetic damping force feedback adjustment to reduce the difference between the ideal semiactive control force $-c_{sky} \cdot \dot{x}_2$ and the actual semiactive control force, the method is as follows.

When $|c_{sky} \cdot \dot{x}_2| > |F_s|$, the semiactive control force of the hybrid suspension is provided by both the MR damper and the ball screw actuator, and at this point, the controller inputs a controllable current I_k to the MR damper, so that the F_k output by the MR damper is $-c_{sky} \cdot \dot{x}_2 - F_s$. And when $|c_{sky} \cdot \dot{x}_2| \le |F_s|$, the semiactive control force of the hybrid suspension is the F_s which is output by the ball screw actuator, and at this point, there is no controllable current I_k input to the MR damper, and the function of the MR damper is equivalent to a traditional shock absorber. Therefore, the semiactive control of the hybrid suspension does not have the dead zone of traditional electromagnetic semiactive suspension, which helps to improve the semiactive control effect of the hybrid suspension.

When there is feedback adjustment, the semiactive control force of the hybrid suspension is

$$F_b = \begin{cases} F_s, & |F_s| \ge |c_{sky} \cdot \dot{x}_2|, \\ -c_{sky} \cdot \dot{x}_2, & |F_s| < |c_{sky} \cdot \dot{x}_2|. \end{cases} \tag{32}$$

When there is feedback adjustment, the F_k output by the MR damper is

$$F_k = \begin{cases} 0, & |F_s| \ge |c_{sky} \cdot \dot{x}_2|, \\ -c_{sky} \cdot \dot{x}_2 - F_s, & |F_s| < |c_{sky} \cdot \dot{x}_2|. \end{cases} \tag{33}$$

From equations (31)~(33), when the electromagnetic damping force feedback adjustment is used, the $|F_k|$ output by the MR damper decreases, and when $|F_k|$ decreases, it can be known from equations (8) and (9) that the energy consumption of the MR damper decreases with it.

The comparison of the semiactive control force of the hybrid suspension with or without the electromagnetic damping force feedback adjustment is shown in Figure 15.

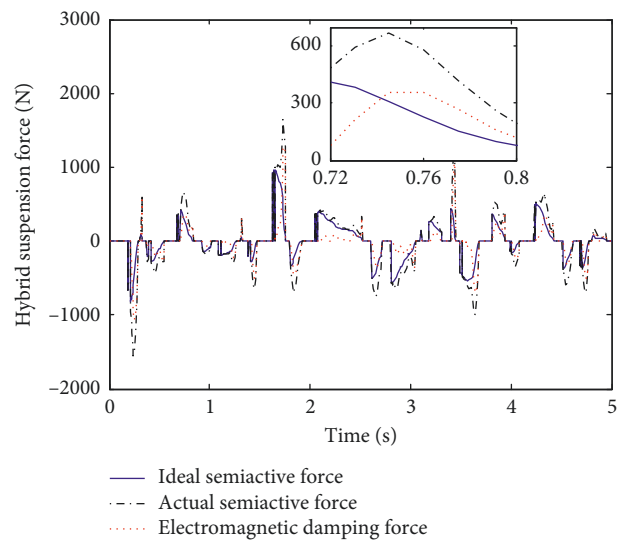

Figure 14: Damping comparison of the hybrid suspension in semiactive control.

From Figure 15, the RMS of the ideal semiactive control force of the hybrid suspension is 327.6 N, and when there is no electromagnetic damping force feedback adjustment, the RMS of the actual semiactive control force of the suspension is 404.1 N, and the difference between the actual semiactive force of the suspension and the ideal semiactive force is 23.35%. When there is electromagnetic damping force feedback adjustment, the RMS of the actual semiactive control force of the suspension is 359.3 N, and the difference between the actual semiactive force of the suspension and the ideal semiactive force is 9.68%. Therefore, when there is electromagnetic damping force feedback adjustment, the actual semiactive control force of the suspension has a smaller fluctuation amplitude, which helps to improve the semiactive control effect of the hybrid suspension.

The dynamic responses of the hybrid suspension with or without electromagnetic damping force feedback adjustment are shown in Figure 16. Among them, the damper of the passive suspension is the original damper of the vehicle, and its damping value is 1600 N·s/m.

Table 2 shows the response RMS values of the hybrid suspension in semiactive control.

From Table 2, compared with the passive suspension, when there is electromagnetic damping force feedback adjustment, a_w, SWS_{rms}, and DTL_{rms} of the hybrid suspension are reduced by 16.98%, 4.32%, and 10.68%, respectively, and compared with the nonfeedback semiactive control, when the feedback semiactive control is performed, a_w, SWS_{rms}, and DTL_{rms} of the hybrid suspension are reduced by 2.52%, 8.63%, and 6.71%, respectively.

From equations (9) and (29), the total system energy of the hybrid suspension in semiactive control is

$$W_1 = W_k - W_b, \tag{34}$$

where W_1 is the total system energy of the hybrid suspension in semiactive control.

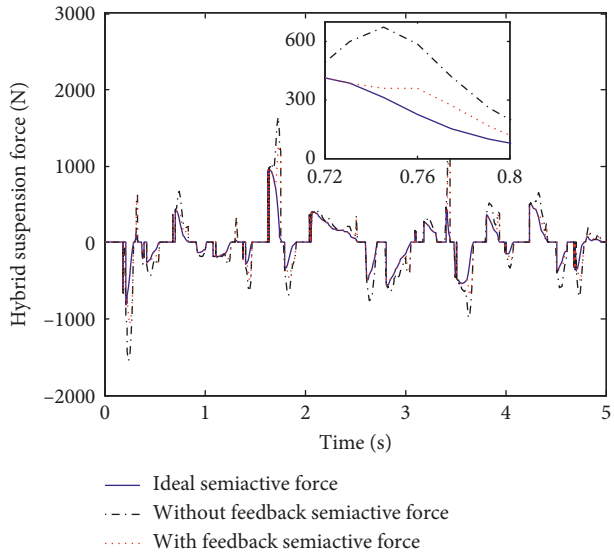

Figure 15: Semiactive force of the hybrid suspension.

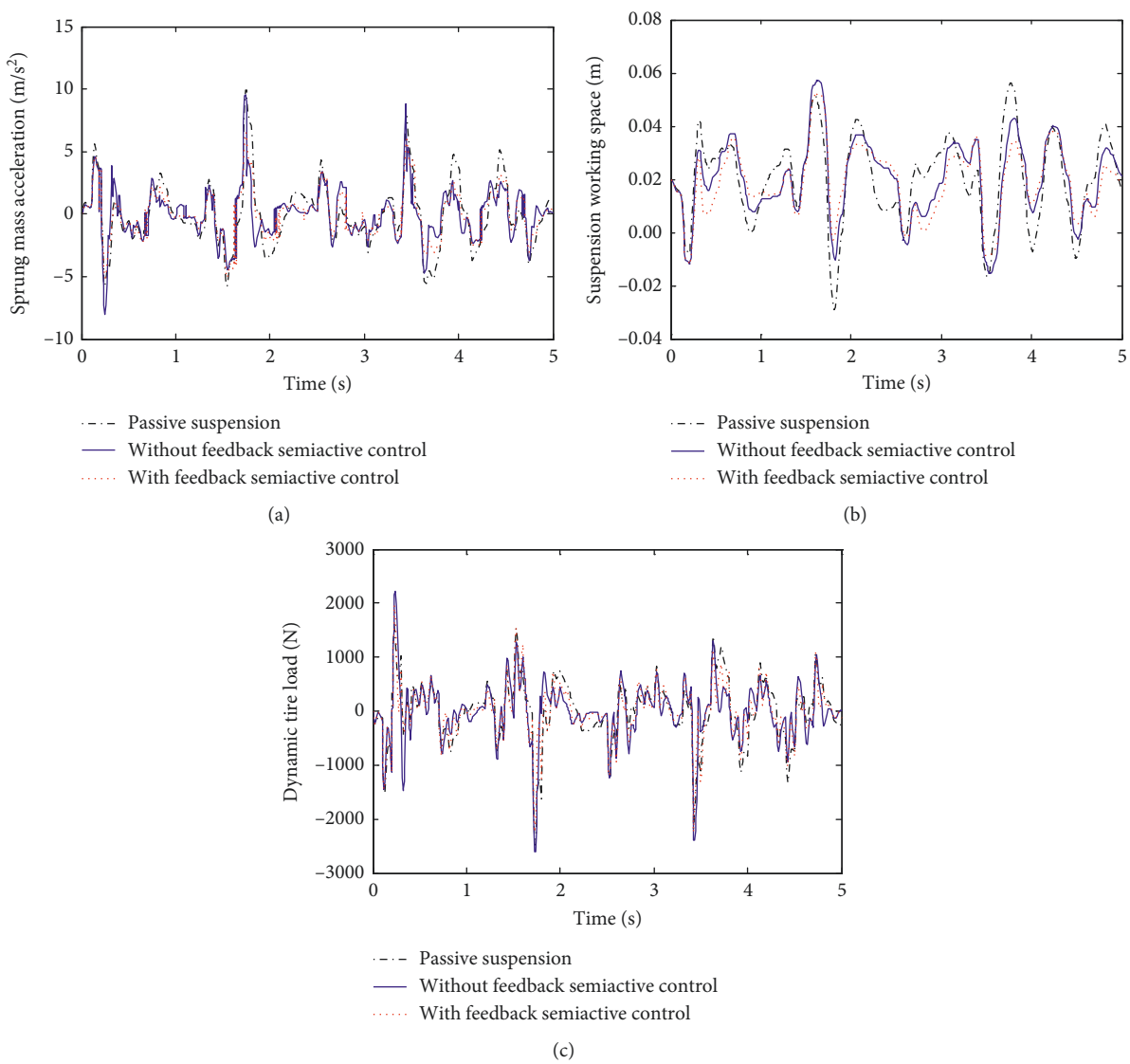

Figure 16: The dynamic responses of the hybrid suspension in semiactive control. (a) The response curves of sprung mass acceleration. (b) The response curves of suspension working space. (c) The response curves of dynamic tire load.

Table 2: The response root mean square values of the hybrid suspension in semiactive control.

Indicators	Passive suspension	Without feedback semiactive control	With feedback semiactive control
a_w (m/s^2)	2.3638	2.0133	1.9625
SWSrms (m)	0.0185	0.0194	0.0177
DTLrms (N)	505.0077	481.3326	451.0680

From equation (33), when the hybrid suspension semiactive controlled, the curves of the total system energy change over time are shown in Figure 17.

From Figure 17, when there is the nonfeedback semiactive control, the total system energy of the hybrid suspension is 60 J. And when there is the feedback semiactive control, the total system energy of the hybrid suspension is 307 J.

4.3. The Design of Multimode Coordination Controller. When the hybrid suspension is actively controlled, the suspension has good vibration isolation performance but high energy consumption. And when the hybrid suspension is semiactively controlled, the suspension has good economic performance but the control has limitations. Considering that the ball screw actuator can realize active control of the hybrid suspension in any suspension state, a multimode coordinated control strategy of the hybrid suspension is designed:

$$\begin{cases} \begin{cases} F = F_b = \begin{cases} F_s, & |F_s| \geq |c_{sky} \cdot \dot{x}_2|, \\ -c_{sky} \cdot \dot{x}_2, & |F_s| > |c_{sky} \cdot \dot{x}_2|, \end{cases} \\ c_s = c_0, \end{cases} & (\dot{x}_2 - \dot{x}_1)\dot{x}_2 > 0, \\ \begin{cases} F = F_z = -c_{sky} \cdot \dot{x}_2, \\ c_s = c_0 + c_k, \end{cases} & (\dot{x}_2 - \dot{x}_1)\dot{x}_2 \leq 0, \end{cases} \tag{35}$$

The frame diagram of the multimode coordinated control strategy of the hybrid suspension is shown in Figure 18.

From equations (9), (12), (26), and (29), the total system energy of the hybrid suspension in multimode coordinated control is

$$W_2 = W_k - W_b - W_Z - W_c, \tag{36}$$

where W_2 is the total system energy of the hybrid suspension in multimode coordinated control.

A hybrid active suspension simulation model is established by using MATLAB/Simulink software. From Figure 11, when the hybrid suspension is actively controlled, the energy consumption of the MR damper is mainly affected by the vehicle speed. In order to verify the vibration isolation performance and energy consumption performance of the hybrid active suspension in the cyclic driving conditions, this article simulates vehicle urban and suburban conditions which is based on GB/T 19233-2003 "Light Vehicle Fuel Consumption Test Method"; among them, the urban conditions include four cycle units, each cycle time is 195 s; the suburban conditions include one cycle unit, and the cycle time is 400 s [26]. And the schematic diagram of the urban conditions unit is shown in Figure 19.

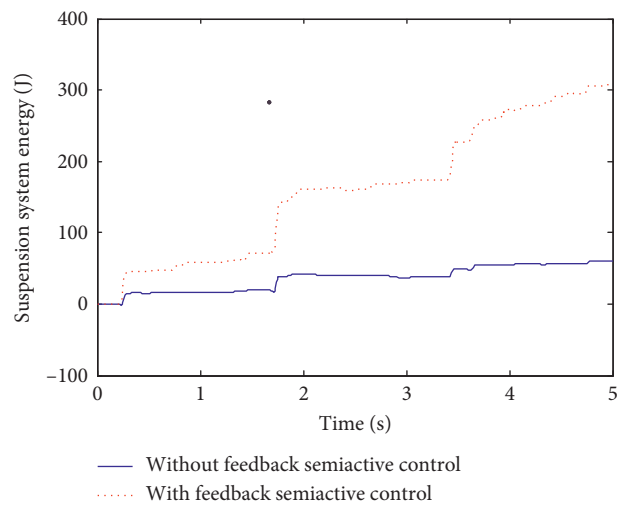

Figure 17: The system energy of the hybrid suspension in semiactive control.

In order to simulate the vehicle acceleration signal, a vehicle speed variation model in different cycle units is established by using the signal builder function module in Simulink software. On this basis, the vehicle acceleration model in different cycle units is obtained, and the vehicle acceleration model can be used as the switching control model for the variable damping when the hybrid suspension is actively controlled. The shock absorbers of active suspension and passive suspension adopt the original damper of vehicle, and the damping value c_1 is 1600 N·s/m. However, because of the long simulation time, the dynamic response curves of the hybrid active suspension in urban and suburban conditions cannot be displayed. Figure 20 shows the dynamic response curve of the hybrid active suspension in the 145–175 s in the urban circulation unit; among them, vehicle in the 145–155 s is in a constant speed, vehicle in the 155–163 s is in the deceleration state, and vehicle in the 163–175 s is in other constant speed.

The dynamic response RMS values of the hybrid suspension in urban and suburban circulation units are shown in Tables 3 and 4, respectively.

From Figure 20 and Tables 3 and 4, the dynamic responses are good when the hybrid suspension is multimode coordinated control. When in the urban circulation unit, compared with the passive suspension, a_w, SWS_{rms}, and DTL_{rms} of the hybrid suspension are reduced by 39.43%, 2.25%, and 20.81%, respectively. Compared with the active suspension, a_w and DTL_{rms} of the hybrid suspension are reduced by 13.22% and 8.40%, respectively, but SWS_{rms} is increased by 8.05%. When in the suburban circulation unit, compared with the passive suspension, a_w, SWS_{rms}, and DTL_{rms} of the hybrid suspension are reduced by 39.16%, 3.14%, and 19.55%, respectively. Compared with the active suspension, a_w and DTL_{rms} of the hybrid suspension are reduced by 11.99% and 7.32%, respectively, but SWS_{rms} is increased by 8.45%.

The system energy of the hybrid suspension in urban and suburban circulation units are shown in Figures 21 and 22, respectively.

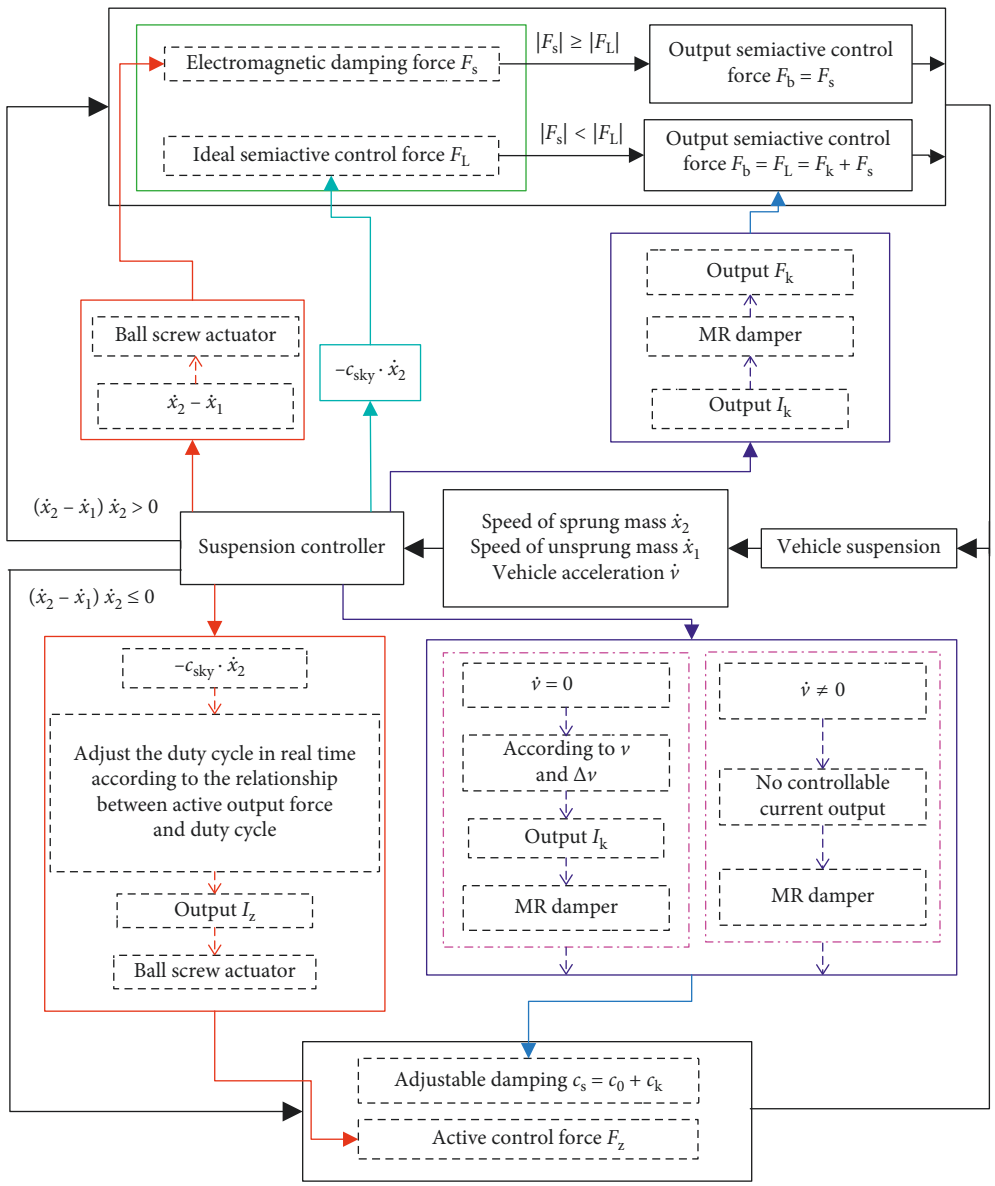

Figure 18: The frame diagram of the multimode coordinated control strategy of the hybrid suspension.

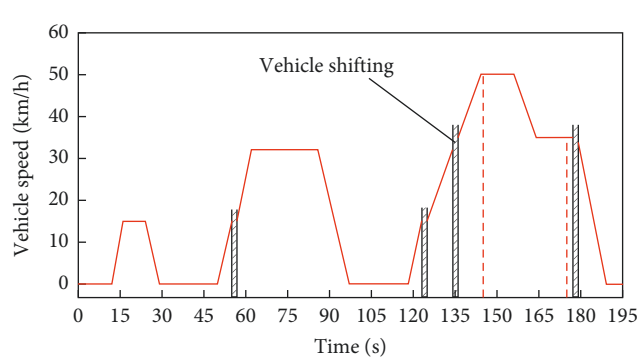

Figure 19: The schematic diagram of the urban conditions unit.

Then, the system energy values of the hybrid suspension in urban and suburban circulation units are shown in Table 5.

From Table 5, when in the urban circulation unit, the system energy of the active suspension and hybrid suspension is −2165 J and 38 J, respectively. And when in the suburban circulation unit, the system energy of the active suspension and hybrid suspension is −15071 J and −122 J, respectively. The entire operation cycle includes 4 urban cycle units and 1 suburban cycle unit, so the pure energy of the active suspension system during the entire operation cycle is −23731 J, while the pure energy of the hybrid suspension system is 38 J. Therefore, the hybrid suspension system basically realizes energy self-powered in theory.

5. Test and Analysis

In order to verify the damping effect of the hybrid suspension system in active mode and semiactive mode, a hybrid suspension vibration test system is designed, as

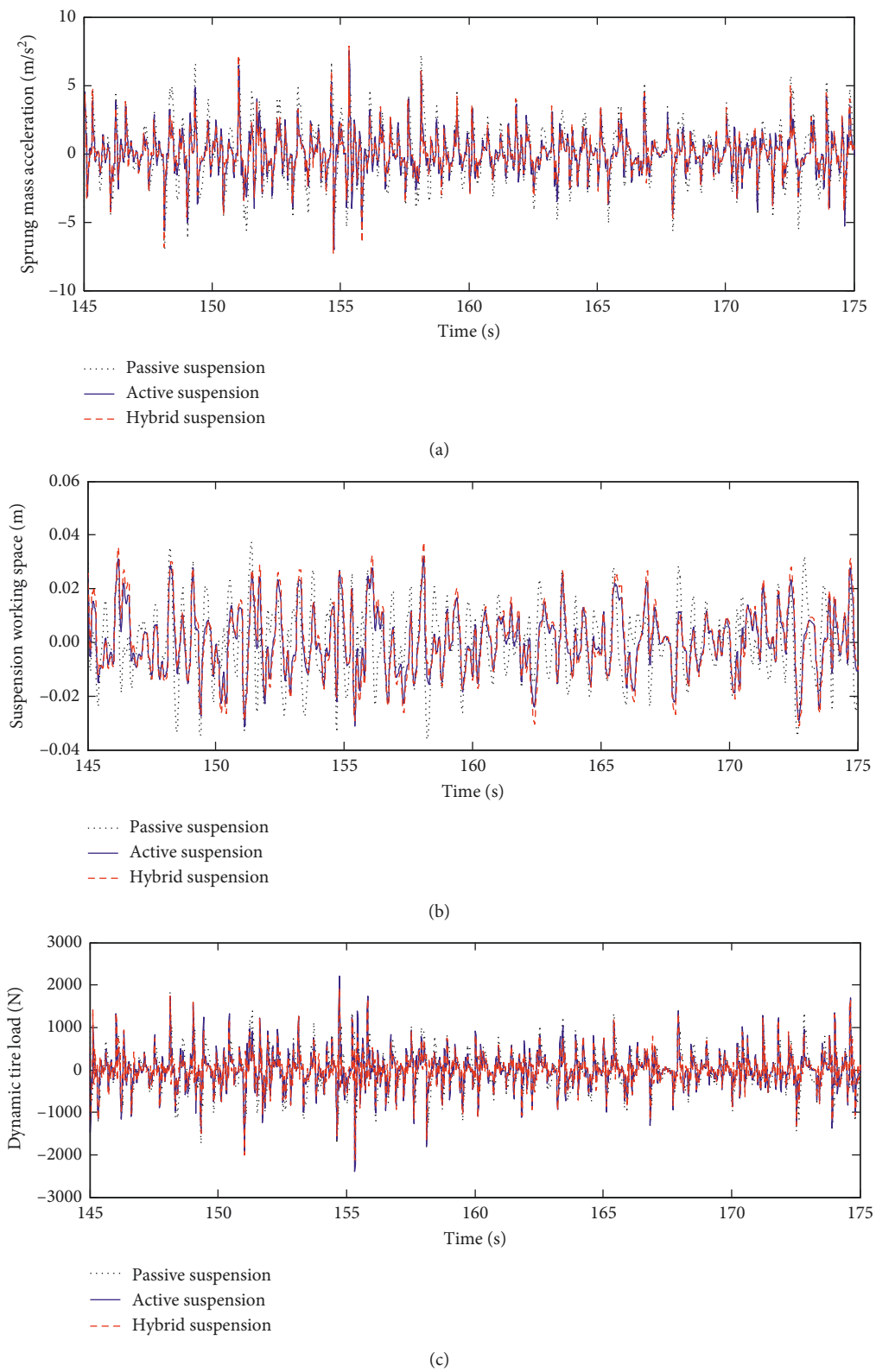

Figure 20: The dynamic responses of the hybrid suspension. (a) The response curves of sprung mass acceleration. (b) The response curves of suspension working space. (c) The response curves of dynamic tire load.

shown in Figure 23. During the test, the MR damper has no controllable current input in the active control mode of the hybrid suspension, and its damping value is always 800 N·s/m. The passive suspension, semiactive suspension, and active suspension all adopt the original damper of the vehicle, and the damping value c_1 is 1600 N·s/m.

Table 3: The dynamic response root mean square values of the hybrid suspension in urban circulation unit.

Indicators	Passive suspension	Active suspension	Hybrid suspension
a_w (m/s^2)	1.4440	1.0078	0.8746
SWS_{rms} (m)	0.0089	0.0080	0.0087
DTL_{rms} (N)	334.4223	289.1024	264.8285

Table 4: The dynamic response root mean square values of the hybrid suspension in suburban circulation unit.

Indicators	Passive suspension	Active suspension	Hybrid suspension
a_w (m/s^2)	2.5204	1.7422	1.5333
SWSrms (m)	0.0159	0.0142	0.0154
DTLrms (N)	585.4460	508.2344	470.9650

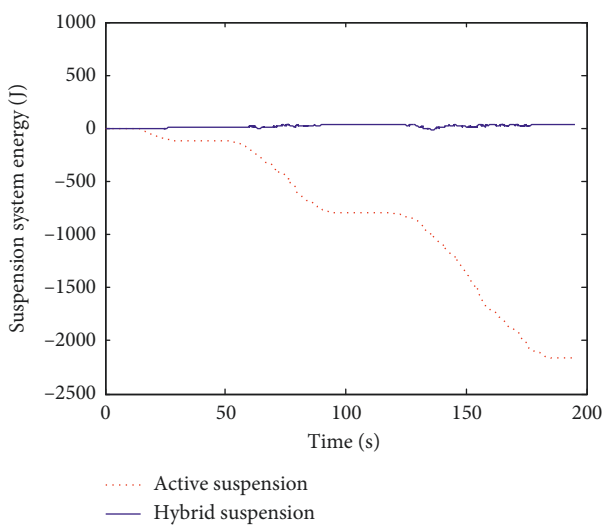

Figure 21: The system energy of the hybrid suspension in urban circulation units.

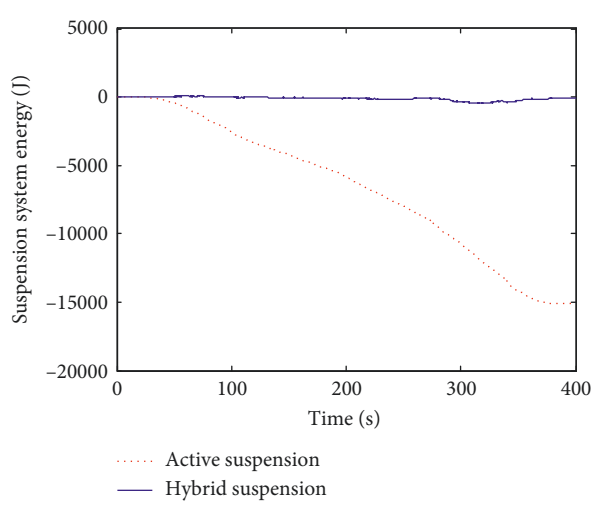

Figure 22: The system energy of the hybrid suspension in suburban circulation units.

Table 5: The system energy values of the hybrid suspension (J).

Cycle unit	Active suspension	Hybrid suspension
Urban	−2165	38
Suburban	−15071	−122

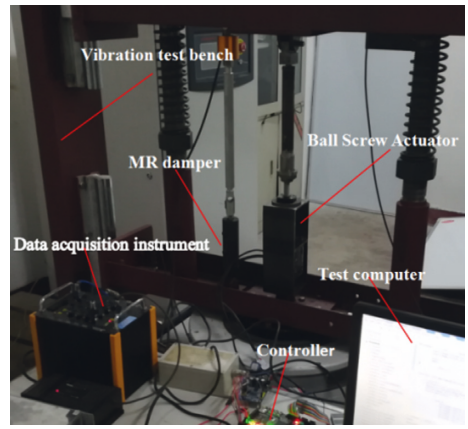

Figure 23: The test system of the hybrid active suspension.

Because of the limitation of test conditions, only the sprung mass acceleration dynamic response of the hybrid suspension is measured in this test. The dynamic response of the sprung mass acceleration of the hybrid suspension in active mode under random road is shown in Figure 24. The power spectrum of the sprung mass acceleration of the hybrid suspension in active mode is shown in Figure 25.

Table 6 shows the sprung mass acceleration RMS test values of the hybrid suspension in active mode.

From Table 6, compared with passive suspension, a_w of the hybrid suspension in active mode is reduced by 39.45%, and compared with active suspension, a_w of the hybrid suspension in active mode is reduced by 14.32%. And from Figure 25, when the hybrid suspension is actively controlled, compared with passive suspension, the vibration isolation performance of the suspension in the low frequency and low-frequency resonance areas is similar to that of the passive suspension, and the vibration isolation performance in the high frequency and high-frequency resonance areas is better than that of the passive suspension. Compared with active suspension, the vibration isolation performance of the suspension in the low frequency, high frequency, and resonance regions is slightly better.

The dynamic response of the sprung mass acceleration of the hybrid suspension in semiactive mode under random road is shown in Figure 26. The power spectrum of the sprung mass acceleration of the hybrid suspension in semiactive mode is shown in Figure 27.

Table 7 shows the sprung mass acceleration RMS test values of the hybrid suspension in semiactive mode.

From Table 7, compared with passive suspension, a_w of the hybrid suspension in semiactive mode is reduced by 16.42%. Compared with semiactive suspension, a_w of the hybrid suspension in active mode is reduced by 3.07%. And from Figure 27, when the hybrid suspension is semiactively controlled, compared with passive suspension, the vibration

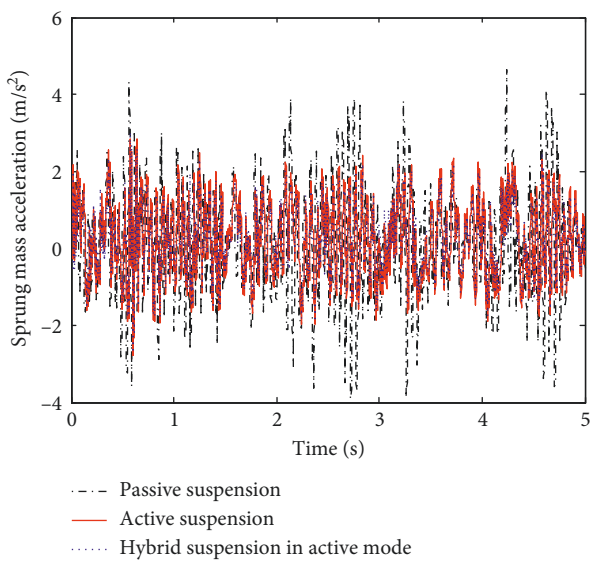

Figure 24: The dynamic response of the sprung mass acceleration of the hybrid suspension in active mode.

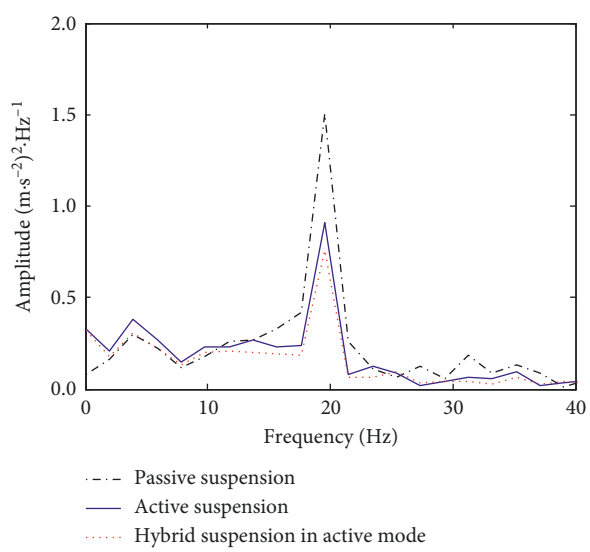

Figure 25: The power spectrum of the sprung mass acceleration of the hybrid suspension in active mode.

Table 6: The sprung mass acceleration RMS of the hybrid suspension in active mode.

Indicators	Passive suspension	Active suspension	Hybrid suspension
a_w (m/s^2)	1.3378	0.9423	0.8074

isolation performance of the suspension in the low frequency and low-frequency resonance areas is worse than that of the passive suspension, and the vibration isolation performance in the high frequency and high-frequency resonance areas is better than that of the passive suspension. Compared with semiactive suspension, the vibration isolation performance of the suspension in the low frequency, high frequency, and resonance regions is slightly better.

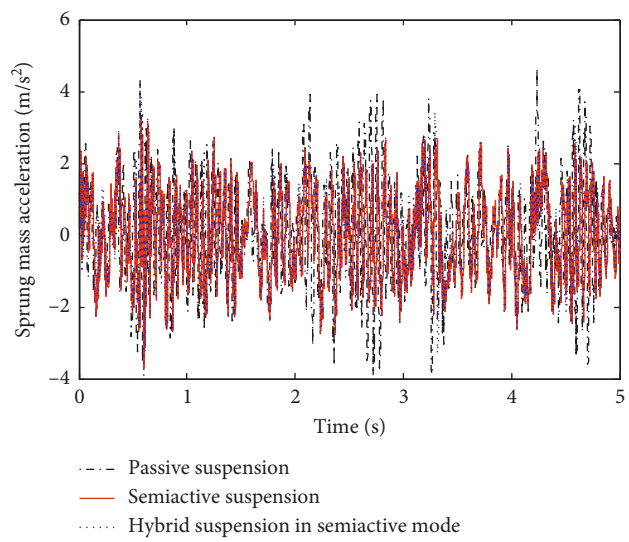

Figure 26: The dynamic responses of the sprung mass acceleration of the hybrid suspension in semiactive mode.

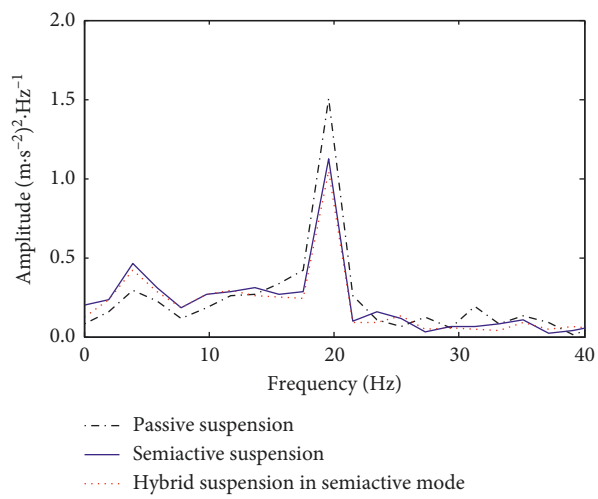

Figure 27: The power spectrums of the sprung mass acceleration of the hybrid suspension in semiactive mode.

Table 7: The sprung mass acceleration RMS of the hybrid suspension in semiactive mode.

Indicators	Passive suspension	Semiactive suspension	Hybrid suspension
a_w (m/s^2)	1.3378	1.1536	1.1182

The energy consumption power and energy-regenerative power of the hybrid suspension are shown in Figure 28.

From Figure 28, in the active mode, the average power consumption of the ball screw actuator is 25.61 W. In the semiactive mode, the average regenerative power of the ball screw actuator is 26.96 W, and the average of the MR damper energy consumption power is 1.78 W. Therefore, the pure average power consumption of the hybrid suspension is −0.43 W, and the test results are basically consistent with the simulation.

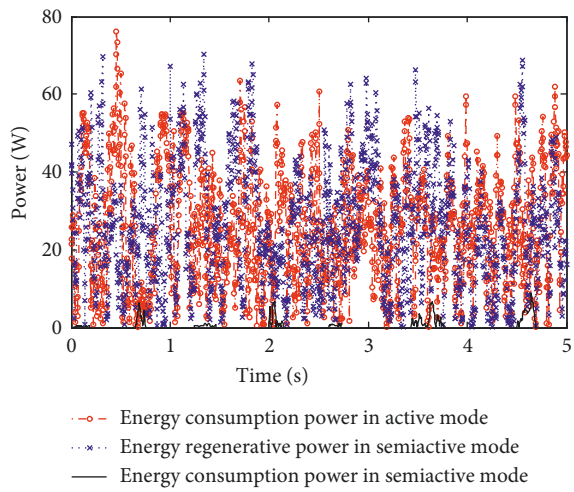

Figure 28: The energy consumption power and energy-regenerative power of the hybrid suspension.

6. Conclusion

(1) A ball screw actuator and MR damper are introduced into vehicle suspension system and a new kind of hybrid active suspension structure is put forward. The ball screw actuator is prototyped, and the functional relationship between the back-EMF coefficient, the electromagnetic torque coefficient of the motor, and the suspension vibration speed is obtained by test analyses. And the active output mechanical properties of the ball screw actuator are tested, and the results show that the actuator has good active output force characteristics.

(2) The influences of the variable damping value of the suspension system on the riding comfort, handling and stability, and energy consumption characteristics of the hybrid suspension in the active control mode are analyzed. Then, the optimal damping values of the hybrid suspension at different vehicle speeds are designed. The effects of electromagnetic damping force on the actual semiactive force and the system energy of the suspension in the semiactive control mode are analyzed, and then, the hybrid suspension with semiactive mode which has electromagnetic damping force feedback adjustment is designed. On this basis, a multimode coordinated control strategy for the hybrid suspension is designed.

(3) The damping performance and energy consumption characteristics of the hybrid suspension under cyclic driving condition are simulated by MATLAB/Simulink software, and the results show that when in the urban circulation unit, compared with active suspension, a_w and DTL_{rms} of the hybrid suspension are reduced by 13.22% and 8.40%, respectively. And when in the suburban circulation unit, compared with the active suspension, a_w and DTL_{rms} of the hybrid suspension are reduced by 11.99% and 7.32%, respectively. The pure energy of the active suspension system during the entire operation cycle is −23731 J, while the pure energy of the hybrid suspension system is 38 J. Therefore, the hybrid suspension system basically realizes energy self-powered in theory.

(4) The effectiveness verification test of the hybrid suspension in active mode and semiactive mode control is carried out, and the results show that when the hybrid suspension is actively controlled, compared with active suspension, a_w of the hybrid suspension in active mode is reduced by 14.32%. When the hybrid suspension is semiactively controlled, compared with semiactive suspension, a_w of the hybrid suspension in active mode is reduced by 3.07%. The test and simulation results are basically consistent, and the test verifies the correctness of the simulation.

Data Availability

The data used to support the findings of this study are included within the supplementary information files. And the data used to support the findings of this study are available from the corresponding author upon request.

Conflicts of Interest

The authors declare that there are no conflicts of interest regarding the publication of this paper.

Acknowledgments

This work was supported by the National Natural Science Foundation of China (Grant no. 51775426), Service Local Special Program Support Project of Shaanxi Provincial Education Department (Grant no. 17JF017), and Xi'an Science and Technology Program Funding Project (Grant no. 2017079CG/RC042-XAKD007).

Supplementary Materials

The supplementary materials are this article's experimental data, including (1) MR damper's characteristic test data; (2) the motor counter electromotive force's peak test data; (3) the ball screw actuator's active output force test data; (4) the hybrid suspension's sprung mass acceleration test data in active mode; (5) the hybrid suspension's sprung mass acceleration test data in semiactive mode; and (6) the hybrid suspension's energy consumption power and energy regeneration power test data. (*Supplementary Materials*)

References

[1] M. Montazeri-Gh and O. Kavianipour, "Investigation of the active electromagnetic suspension system considering hybrid control strategy," *Proceedings of the Institution of Mechanical Engineers, Part C: Journal of Mechanical Engineering Science*, vol. 228, no. 10, pp. 1658–1669, 2013.

[2] H. E. Tseng and D. Hrovat, "State of the art survey: active and semi-active suspension control," *Vehicle System Dynamics*, vol. 53, no. 7, pp. 1034–1062, 2015.

[3] F. Kou, J. Du, Z. Wang, D. Li, and J. Xu, "Nonlinear modeling and coordinate optimization of a semi-active energy regenerative suspension with an electro-hydraulic actuator," *China Mechanical Engineering*, vol. 28, no. 14, pp. 1701–1707, 2017.

[4] S. H. Zareh, A. Sarrafan, A. A. A. Khayyat, and A. Zabihollah, "Intelligent semi-active vibration control of eleven degrees of freedom suspension system using magnetorheological dampers," *Journal of Mechanical Science and Technology*, vol. 26, no. 3, pp. 323–334, 2012.

[5] S. A. Chen, X. Li, L. J. Zhao, Y. X. Wang, and Y. B. Kim, "Development of a control method for an electromagnetic semi-active suspension reclaiming energy with varying charge voltage in steps," *International Journal of Automotive Technology*, vol. 16, no. 5, pp. 765–773, 2015.

[6] K. Nakano, Y. Suda, and S. Nakadai, "Self-powered active vibration control using a single electric actuator," *Journal of Sound and Vibration*, vol. 260, no. 2, pp. 213–235, 2003.

[7] K. Nakano, "Combined type self-powered active vibration control of truck cabins," *Vehicle System Dynamics*, vol. 41, no. 6, pp. 449–473, 2004.

[8] K. Huang, Y. C. Zhang, F. Yu, and Y. H. Gu, "Coordinate optimization for synthetical performance of electrical energy-regenerative active suspension," *Journal of Shanghai Jiaotong University*, vol. 43, no. 2, pp. 226–230, 2009.

[9] K. Huang, F. Yu, and Y. C. Zhang, "Active control of energy-regenerative electromagnetic suspension based on energy flow analysis," *Journal of Shanghai Jiaotong University*, vol. 45, no. 67, pp. 1068–1073, 2011.

[10] D. S. Huang, J. Q. Zhang, Y. L. Liu, L. Yi, and X. Y. Wang, "Performance of a novel energy-regenerative active suspension system," *Journal of Chongqing University (English Edition)*, vol. 14, no. 3, pp. 109–118, 2015.

[11] B. Ebrahimi, H. Bolandhemmat, M. B. Khamesee, and F. Golnaraghi, "A hybrid electromagnetic shock absorber for active vehicle suspension systems," *Vehicle System Dynamics*, vol. 49, no. 1-2, pp. 311–332, 2011.

[12] S. Tang, L. Chen, R. Wang, X. Sun, and D. Shi, "Research on optimal control of active suspension based on damping multi-modal switching," *Journal of Guangxi University (Natural Science)*, vol. 39, no. 2, pp. 300–307, 2014.

[13] R. Wang, X. Ma, R. Ding, X. Meng, and L. Chen, "Research of multi-mode switching control system for hybrid suspension based on model reference," *Transactions of the Chinese Society for Agricultural Machinery*, vol. 48, no. 7, pp. 353–360, 2017.

[14] R. Wang, Y. Qian, R. Ding, X. Meng, and J. Xie, "Design and tests for damping-stiffness of a hybrid electromagnetic suspension based on LQG," *Journal of Vibration and Shock*, vol. 37, no. 3, pp. 61–65, 2017.

[15] B. Vanavil, K. K. Chaitanya, and A. S. Rao, "Improved PID controller design for unstable time delay processes based on direct synthesis method and maximum sensitivity," *Taylor and Francis*, vol. 46, no. 8, pp. 1349–1366, 2015.

[16] I. Mihai and F. Andronic, "Behavior of a semi-active suspension system versus a passive suspension system on an uneven road surface," *Mechanics*, vol. 20, no. 1, pp. 64–69, 2014.

[17] D. Ngoduy, "Linear stability of a generalized multi-anticipative car following model with time delays," *Communications in Nonlinear Science and Numerical Simulation*, vol. 22, no. 1, pp. 420–426, 2015.

[18] H. Zhang, E. Wang, F. Min, R. Subash, and C. Su, "Skyhook-based semi-active control of full-vehicle suspension with magneto-rheological dampers," *Chinese Journal of Mechanical Engineering*, vol. 26, no. 3, pp. 498–505, 2013.

[19] F. Kou, "An experimental study on the dynamic characteristics of vehicle semi-active seat suspension with magneto-rheological damper," *Automotive Engineering*, vol. 37, no. 11, pp. 1346–1352, 2015.

[20] Z. Feng, S. Chen, and Y. Liang, "An experimental study on the dynamic characteristics of a megneto-rheological semi-active suspension," *Automotive Engineering*, vol. 35, no. 1, pp. 72–77, 2013.

[21] Z. Li and L. Xu, *A New Type of Magnetorheological Damper and Semi-Active coNtrol Design Theory*, Science Press, Beijing, China, 2012.

[22] B. L. J. Gysen, J. J. H. Paulides, J. L. G. Janssen, and E. A. Lomonova, "Active electromagnetic suspension system for improved vehicle dynamics," *IEEE Transactions on Vehicular Technology*, vol. 59, no. 3, pp. 1156–1163, 2010.

[23] Q. N. Wang, S. S. Liu, W. H. Wang, and H. Wei, "Structure design and parameter matching of ball-screw regenerative damper," *Journal of Jilin University (Engineering and Technology Edition)*, vol. 42, no. 5, pp. 1100–1106, 2012.

[24] S. Chen, R. He, and S. Lu, "Evaluating system of reclaiming energy suspension comprehensive performance," *Transactions of the Chinese Society for Agricultural Machinery*, vol. 37, no. 7, pp. 14–18, 2006.

[25] Y. Fan, *Control Research on Vehicle Suspension with Electro-Hydrostatic Actuator*, Xi'an University of Science and Technology, Xi'an, China, 2017.

[26] Z. Yu, *Automobile Theory*, China Machine Press, Beijing, China, 2009.